Published in final edited form as:
*Cancer Res*. 2011 February 1; 71(3): 852–861. doi:10.1158/0008-5472.CAN-10-1219.

# miRNA-7 attenuation in schwannoma tumors stimulates growth by upregulating three oncogenic signaling pathways

**Okay Saydam**[1,*], **Ozlem Senol**[1], **Thomas Würdinger**[1,**], **Arda Mizrak**[1], **Gokhan Baris Ozdener**[1], **Anat O. Stemmer-Rachamimov**[2], **Ming Yi**[3], **Robert M. Stephens**[3], **Anna M. Krichevsky**[4], **Nurten Saydam**[5], **Gary J. Brenner**[6], and **Xandra O. Breakefield**[1]

[1]Departments of Neurology and Radiology, Massachusetts General Hospital, and Neuroscience Program, Harvard Medical School, Boston, Massachusetts, 02129 USA

[2]Molecular Neuro-oncology Laboratory and Department of Pathology, Massachusetts General Hospital, Harvard Medical School, Boston, Massachusetts, 02129 USA

[3]Advanced Biomedical Computing Center, National Cancer Institute, Bethesda, Maryland, 21702 USA

[4]Department of Neurology, Brigham and Women's Hospital, Harvard Medical School, Boston, MA, 02115 USA

[5]Department of Pediatrics, Medical University of Vienna, 1090 Austria

[6]Department of Anesthesia and Critical Care, Massachusetts General Hospital, Harvard Medical School, Boston, MA

## Abstract

MicroRNAs (miRNAs) negatively regulate protein-coding genes at the post-transcriptional level and are critical in tumorigenesis. Schwannomas develop from proliferation of dedifferentiated Schwann cells, which normally wrap nerve fibers to help support and insulate nerves. In this study, we carried out high-throughput miRNA expression profiling of human vestibular schwannomas using an array representing 407 known miRNAs in order to explore the role of miRNAs in tumor growth. Twelve miRNAs were found to be significantly deregulated in tumor samples as compared with control nerve tissue, defining a schwannoma-typical signature. Among these miRNAs, we focused on miR-7 which was one of the most downregulated in these tumors and has several known oncogene targets, including mRNAs for epidermal growth factor receptor (EGFR) and p21-activated kinase 1 (Pak1). We found that overexpression of miR-7 inhibited schwannoma cell growth both in culture and in xenograft tumor models in vivo, which correlated with downregulation of these signaling pathways. Furthermore, we identified a novel direct target of miR-7, the mRNA for associated cdc42 kinase 1 (Ack1), with the expression levels of miR-7 and Ack1 being inversely correlated in human schwannoma samples. These results represent the first miRNA profiling of schwannomas and the first report of a tumor suppressor function for miR-7 in these tumors that is mediated by targeting the EGFR, Pak1 and Ack1 oncogenes. Our findings suggest miR-7 as a potential therapeutic molecule for schwannoma treatment, and they prompt clinical evaluation of drugs that can inhibit the EGFR, Pak1, and Ack1 signaling pathways to treat this tumor type.



[*]Corresponding author and requests for reprints: Okay Saydam, Ph.D., Department of Pediatrics, Medical University of Vienna, 1090 Austria. Phone: 43-1-404003232 8, okay.saydam@meduniwien.ac.at.
[*]Current address for O. Saydam: Department of Pediatrics, Medical University of Vienna, 1090 Austria
[**]Current address for T. Würdinger: Neuro-oncology Research Group, Department of Neurosurgery, VU University Medical Center, Amsterdam 1007 MB, The Netherlands

**Keywords**

miRNAs; schwannomas; Ack1; EGFR; Pak1

## INTRODUCTION

Schwannomas arise from Schwann cells, the myelinating cells of the peripheral nervous system and they typically result from loss of the neurofibromatosis 2 (*NF2*) tumor suppressor gene (1), but can also arise through other genetic mechanisms, such as inactivating mutations in *PRKAR1A* (2) or loss of heterozygosity (LOH) of *SMARCB1* (3) genes. A major feature of NF2 is the development of schwannomas around the vestibular branches of cranial nerve VIII, the auditory nerve, leading to deafness (4). Loss/downregulation of NF2 has also been found in malignant tumors, including mesotheliomas (5), gliomas (6), peripheral nerve sheath tumors (7), and prostate cancer (8).

miRNAs are a class of small non-coding RNAs that regulate gene expression post-transcriptionally (9). miRNAs have been recently implicated as drivers in several carcinogenic processes, where they can act either as oncogenes or as tumor suppressors (10). Decreased levels of the let-7 family of tumor suppressor miRNAs is associated with increased Ras oncogene expression and reduced survival in patients with non-small cell lung cancer (NSCLC) (11,12). Our recent studies revealed a novel potential tumor suppressor miRNA, miR-200a, which directly targets the β-catenin and ZEP1/SIP1 mRNAs, with reduced levels of miR-200a found in meningiomas (also caused in some cases by loss of merlin function) resulting in increases in Wnt signaling and expression of E-cadherin (13).

Previously known targets for miR-7 include messages for signaling proteins, Pak1 (14) and epidermal growth factor receptor (EGFR) (15), known to be activated in many forms of cancer. Paks play an essential role in a variety of cellular functions including cell division, survival, angiogenesis, growth factor signaling and cell migration (16–18). A new target for miR-7, found in this study, associated cdc42 kinase 1 (Ack1) is a non-receptor protein tyrosine kinase (19), and the gene encoding Ack1 has been recently shown to be amplified in breast, esophageal, lung, ovarian, pancreatic, and prostate cancer (20).

To identify miRNAs signature of schwannomas, we analyzed the expression levels of 407 human miRNAs in human vestibular schwannoma tumor samples compared to normal control nerve tissue. Several previously described potential tumor suppressor miRNAs (let-7, miR-451, miR-23 and miR-29) that are downregulated in malignant tumors (reviewed in 21,22) were found to be upregulated in benign schwannomas, suggesting that changes in levels of tumor suppressor miRNAs may play a transition role from benign to malignant tumors. miR-7 was found to be one of the most downregulated miRNAs (~9-fold) in schwannomas compared to control nerves. To explore the role of miR-7 in schwannomas, we performed gain-of-function studies and found that upregulation of miR-7 inhibited schwannoma cell growth both in culture and in xenograft tumors model *in vivo*. Moreover, overexpression of miR-7 directly targeted and inhibited expression of Ack1, Pak1, and EGFR in schwannoma cells.

## MATERIALS AND METHODS

### Tumor and normal tissue samples

Human vestibular schwannoma tumor samples were obtained from discarded tumor tissue at the time of surgery and normal peripheral nerve tissue samples were obtained from fresh autopsy cases within 5–7 h of death. All human tissues were collected and de-identified by

the Neuro-oncology Tumor Repository, snap-frozen and stored at −80°C under IRB protocols approved by Massachusetts General Hospital Committee on Human Research.

### Cells

Human schwannoma cell line HEI-193 was established from a benign schwannoma tumor from an NF2 patient and immortalized using a retrovirus vector encoding HPV E6–E7 (obtained from the House Ear Institute in 2006; 1). Before we initiated this study, we confirmed a G to A conversion at the −1 position of the intron 14/exon 15 border of the *NF2* gene in HEI-193 cells (data not shown), which eliminates a splice donor site and generates a non-functional NF2 protein (23). These cells were transduced with lentivirus vector expressing firefly luciferase (Fluc) and mCherry genes, termed HEI-193-Fluc-mC cells, as described (13) and were cultured, as described (1) and used in *in vivo* studies. Human primary schwannoma cell cultures were prepared in our laboratory from fresh tumor tissue from a schwannoma patient, as described (23) during the revision of this manuscript in 2010. The NF2S-1 mouse schwannoma cell line was generated and characterized by our laboratory in 2006, as described (24) and used at early passages (passage number P6 was used in our studies). These cells were tested for mouse chromosomes by karyotyping: NF2S-1 cells were harvested and metaphase spreads were stained by Giemsa-Trypsin-Giemsa banding and evaluated by the Dana Farber/Harvard Cancer Center Cytogenetics Core Laboratory (Boston, USA) in 2006. All cell lines showed strong immunocytochemical staining for the Schwann cell marker, S100. All cells tested negative for mycoplasma using a mycoplasma detection kit (MycoAlert® Mycoplasma Detection Assay: Lonza, Rockland, ME) before and after use in these experiments.

### Growth rate

HEI-193 cells ($1 \times 10^5$) were seeded in each well of a 24-well plate and the following day transfected with precursor miRNAs or control miRNAs or pre-control 1, or left non-transfected. Five h later, cells were transferred to each well of a 6-well plate. Cells/well were counted on day 1, 2, 3, and 4 using a hemocytometer in triplicate.

### Apoptosis

Apoptotic cell death was determined using the Caspase-Glo 3/7 assay kit (Promega, Madison, WI) and CytoGLO Annexin V-FITC Apoptosis Detection kit (Imgenex, San Diego, CA), according to the manufacturer's instructions.

### miRNAs

Precursor miRNAs were as follows: precursor-miR-7 (Ambion, Foster City, CA, AM17100), precursor-miR-321 (Ambion, AM17153), Cy3 dye-labeled pre-miR negative control 1 (Ambion, AM17120), and pre-miR negative control 1.

### Plasmids/vectors

3'UTR reporter plasmids p3’UTR-EGFR and p3'UTR-IRS-2 containing the full site complementary to miR-7 were kindly provided by Dr. Benjamin Purow (University of Virginia) (15). The following vectors were packaged at the MGH Vector Core facility: Ack1-pWZL Neo Myr Flag TNK2 (Addgene, Cambridge, MA), EGFR-WT Retroviral 11011: (Addgene), and Pak1- EX-T9352-Lv105 (GeneCopoeia, Rockville, MD).

### miRNA arrays

miRNA screening was performed as described previously (13) in duplicate for 10 tumor and 2 control samples. A two-tailed, two-sample *t* test was used with differences of 2-fold or

greater between samples ($p<0.05$) regarded as significant. This microarray data set has been deposited in the NCBI Gene Expression Omnibus with the accession no. GSE24390 (25).

### Tumor implantation and bioluminescence imaging

Five after transfection of HEI-193-Fluc-mC cells, the cells were trypsinized, rinsed, and subcutaneously implanted ($2 \times 10^5$ cells in 100 µl Matrigel) per flank of athymic mice (nu/nu, 5-week-old females; NCI). Sciatic nerve schwannoma tumor model were developed as described previously (26).

### Quantitative RT-PCR

qRT-PCR was performed as described (13). U6 RNA was used as an internal control in all RT-PCR reactions for miRNA.

### Luciferase miRNA target reporter assay

Total cDNA from HEI-193 cells was used to isolate the 3'UTR (453–840 nt) of Ack1 by PCR and then it was cloned into the pMir-reporter plasmid (see suppl. Materials and Methods for the cloning strategies for pMir-reporter plasmids). HEK 293T cells were co-transfected either with the p3'UTR-EGFR or p3'UTR-IRS-2 vectors or pAck1 3'UTR plasmids and pre-miR-7 or pre-control 1. Two days later, the cells were lysed and luciferase activity was measured using a luminometer. An expression cassette for *Renilla* luciferase (pRenilla, Promega) was co-transfected and used to normalize the Fluc values expressed from the 3'UTR report constructs.

See suppl. Materials and Methods for primers and antibodies and Pearson correlation coefficients.

### Immunoblots

Western blots were performed, as described (13). Briefly, cells were transfected with miRNA precursors and after 3 days, cells were harvested and total protein was separated on a SDS–8% polyacrylamide gel and blotted onto nitrocellulose.

### Statistical analysis

All measurements including cell counting, luciferase measurement, and qRT-PCR, were performed in triplicate and the values are expressed as the mean ± S.D.; p values were calculated by using the Student's *t*-test and values of $p<0.05$ were regarded as significant.

## RESULTS

### miRNA expression profile of schwannomas

To explore the possible role(s) of miRNAs in schwannoma pathogenesis, we first performed a microarray-based miRNA screen containing 407 different human miRNA-binding probes comparing 10 human vestibular schwannoma tumor samples (WHO Grade I) to two peripheral nerve controls (obtained from fresh autopsies). Nineteen miRNAs were found which had 3-fold or more differences in levels in most (7 or more) schwannoma tumor samples as compared to control nerves (Supplementary Table 1). To validate the microarray results, selected miRNAs differentially expressed in schwannomas were analyzed by qRT-PCR. Twelve of these deregulated miRNAs were confirmed to be either up (8 miRNAs) or downregulated (4 miRNAs) by 5-fold or more in three independent assays (Fig. 1) using four control samples and 10 randomly selected-schwannoma samples out of 15. Let-7d, miR-451, and miR-23b were the most upregulated miRNAs as compared to control tissues (15–20-fold). Other upregulated miRNAs in the qRT-PCR assay were miR-29, miR-30a,

miR-221, miR-21 and miR-138 (5–10-fold). Four downregulated miRNAs were miR-321 (12-fold), miR-7 (9-fold), miR-373* (6-fold) and miR-638 (6-fold). Our data thus revealed a set of miRNAs which are deregulated in a consistent pattern in most vestibular schwannoma tumor samples providing a schwannoma-specific miRNA signature.

### The effect of dysregulated miRNAs on schwannoma cell growth

Among several interesting miRNAs, we focused on the two most downregulated miRNAs, miR-321 and miR-7, as these have been implicated as potential tumor suppressors (10). Due to difficulty in culturing primary Schwann cells, we compared downregulated miRNA levels in the human schwannoma line, HEI-193 (23) to those in the control nerves used in our microarray screening and qRT-PCRs studies. HEI-193 cells have 6- and 5-fold lower levels of miR-7 and miR-321, respectively, compared to control nerves (Fig. 2A). Transfection of these cells with precursor miRNA - 10 nM pre-miR-321 or 15 nM pre-miR-7 yielded 13- and 15-fold increases in miR-321 and miR-7 levels, respectively, after 5 h (Fig. 2B). These concentrations and time were used in further studies. HEI-193 cells were transfected with pre-miR-321, pre-miR-7 or pre-control 1 and five h after transfection these cells were re-plated and cell counts determined 1, 2, 3 and 4 days later. The growth of HEI-193 cells was significantly reduced by about 70% on day 4 after transfection with pre-miR-7 as compared to control transfected cells (Fig. 2C), while miR-321 had no effect on the growth of these cells. With these small oligonucleotides, the transfection efficiency of HEI-193 cells was 99% as determined by transfection of pre-control 1-Cy3 (Ambion) and fluorescence microscopy (data not shown). The effect of transfection with pre-miR-7 was also tested in a mouse schwannoma cell, NF2S-1, and we observed a pronounced inhibition of cell growth by elevated miR-7 in this cell line (data not shown). Taken together our data demonstrate that increased levels of miR-7 can inhibit the growth of schwannoma cells in culture, consistent with the hypothesis that decreased levels of miR-7 support schwannoma tumor growth.

We next investigated whether the reduced cell numbers in the presence of elevated miR-7 expression were due to arrest of cell division or cell death (15). Activities of caspases-3 and -7 were measured in transfected and non-transfected cell two days after transfection. Pre-miR-7 transfected cells showed a significant increase in caspase3/7 activity as compared to controls and pre-miR-321-transfected cells (Fig. 2D), indicating that elevated miR-7 promotes apoptosis in schwannoma cells. We also found 4- and 7-fold increases in the apoptosis marker, Annexin V in HEI-193 and human primary schwannoma cells, respectively, at two days after transfection with pre-miR-7 compared to control transfected cells (Supplementary Fig. 1).

### miR-7 inhibits schwannoma tumor growth *in vivo*

We further evaluated whether increased levels of miR-7 could inhibit schwannoma tumor growth *in vivo*. HEI-193-Fluc schwannoma cells were transfected either with pre-miR-7 or pre-control 1, and 5 h later implanted subcutaneously into flanks of nude mice ($2 \times 10^5$ cells per injection site; 7 mice per group). Two independent *in vivo* studies were performed. Tumor growth was monitored by *in vivo* bioluminescence imaging on day 1, 5 and 10 after implantation. Schwannoma cells transfected with control precursor, pre-control 1 formed tumors 10 days after implantation, while schwannoma cells transfected with pre-miR-7 failed to grow, with a marked reduction in size at day 10 post-implantation. Bioluminescence images of tumors in these mice in two independent experiments are shown in Figure 3A, with quantification of average of photon counts in Figure 3B. In control groups, *in vivo* imaging was terminated two weeks after implantation due to excessive size of tumors. In the pre-miR-7 treated group, *in vivo* imaging was performed for an additional 6

weeks and none of the mice developed tumors. These data indicate that elevated miR-7 levels in schwannoma cells markedly reduce their ability to form tumors.

We have recently developed a novel imaging-compatible sciatic nerve schwannoma model in which the immortalized human schwannoma cell line, HEI-193, has been stably transduced with fluorescent protein and luciferase reporters and implanted within the sciatic nerve of nude mice (25). We used this model to test whether elevated miR-7 can also inhibit schwannoma tumor growth in an orthotopic tumor model, under parallel experimental conditions to those described above, and found also a significant reduction in photon counts for tumors in pre-miR-7 group as compared to the control group (Supplementary Figure 2). The HEI-193 cell line was immortalized with a retrovirus encoding the human papilloma virus immortalizing proteins, E6–E7 (23). These viral proteins are known to inhibit tumor suppressor activity of p53 and RB proteins (27). It seems probable that dysfunctional RB, which is among the predicted targets of miR-7 (26), might make schwannoma cells more sensitive to the tumor suppressive effect of miR-7. In fact, loss of heterozygosity at the RB locus is seen in a substantial number of vestibular schwannoma samples, implicating loss of RB function in these tumors (28).

## Multiple oncogenic targets of miR-7: ACK1 emerges as a novel target for miR-7

In light of previous observations that miR-7 targets the EGFR and Pak1, and IRS-2 mRNAs (14,15,29), we first tested whether miR-7 targeted messages for EGFR, IRS-2, and Pak1 in schwannomas. Due to their higher transfection efficiency with plasmid DNA, HEK 293T cells were co-transfected with the pEGFR-3'UTR-Reporter or the pIRS-2-3'UTR-Reporter and pre-miR-7 or pre-control 1. These reporter plasmids contain an expression cassette for the Fluc gene fused to the full site complementary 3'UTR of EGFR or IRS-2 mRNAs (15). pRenilla was used to normalized the transfection efficiency in all experiments. Two days after transfection, Fluc activity was measured in cell lysates and normalized to *Renilla* luciferase (Rluc) activity. We observed a significant reduction in the Fluc activity of both pEGFR-3'UTR- and pIRS-2-3'UTR-Reporter transfected cells with pre-miR-7 as compared with pre-control 1 (Supplementary Fig. 3A), confirming that miR-7 targets EGFR and IRS2 mRNAs. In a parallel experiment, we monitored transcript levels of EGFR and IRS-2 by qRT-PCR reactions normalized to levels of GAPDH mRNA (Supplementary Fig. 3B) and found a significant decrease of both EGFR and IRS-2 mRNA levels resulting from increased expression of miR-7.

We also tested whether elevated miR-7 could reduce levels of EGFR and Pak1 in schwannoma cells. We used HEI-193 and human primary schwannoma cells and found that upregulation of miR-7 markedly reduced levels of both EGFR and Pak1 as normalized to actin (Supplementary Fig. 3C).

Based on previous findings describing the intermolecular interactions between Ack1, EGFR and Pak1 (30–32), we investigated whether miR-7 also targets mRNA for Ack1. We analyzed the 3'UTR of Ack1 mRNA for potential binding sites for miR-7 and found three top level computationally predicted target sequences in the 3'UTR of the Ack1 mRNA (26;Fig. 4A). To investigate the interaction between miR-7 and its predicted Ack1 mRNA 3'UTR target sites, we generated a series of reporter vectors containing sequences homologous to the three potential seed sequences for miR in the 3'UTR downstream of a luciferase expression construct (Fig. 4B). These included a sequence with perfect complementarity to all 3 seed miR-7 sequences (pAck1 3'UTR 453–840 nt), and the three isolated wt Ack1 3'UTR sequences, pAck1 A, pAck1 B, and pAck1 C, as well as the same three Ack1 sequences with three point mutations to disrupt miR-7 binding in each of the seed match regions (Fig. 4C, lower case). Co-transfection of the pAck1 3'UTR-wt construct (453–840 nt) and pre-miR-7 resulted in significantly decreased luciferase activity compared

to transfection with pre-control 1 (Fig. 4D). We next investigated the relative contribution of each putative miR-7 target site in the Ack1 3'UTR. miR-7 reduced the expression of all three reporters carrying the different putative target sites A and B, and C, but not of the corresponding mutant (mt) reporters (Fig. 4E). The most significant reduction in luciferase activity was observed for target site C which is the most conserved miR-7 binding site in the 3'UTR of the Ack1 mRNA (26) (Fig. 4E). Target sites A and B resulted in less reduction than site C, but still showed significant reduction. Together, these data indicate that the Ack1 3'UTR is a specific target of miR-7 and that all three predicted miR-7-binding sites in the Ack1 mRNA 3'UTR are likely to be specific and direct targets of miR-7 with a marked total effect on expression. We next examined the effect of miR-7 on the endogenous mRNA and protein levels of Ack1. Human primary schwannoma cells and HEI-193 cells were transfected with either pre-miR-7 or pre-control 1 and two days later, we performed qRT-PCR for mRNA and western blots for the protein expression. We found that miR-7 transfection decreased both mRNA (data not shown) and protein levels (Fig. 4F) of Ack1 compared to GAPDH mRNA and actin in both cell types. Elevated miR-7 levels in a mouse schwannoma cell line, NF2S-1, also produced a marked reduction in the protein levels of Ack1, Pak1, and EGFR (Supplementary Fig. 4).

In order to investigate which target(s) of miR-7 are involved in miR-7 mediated growth inhibition of schwannoma cells, HEI-193 cells were first infected with viral vectors expressing either Ack1 or Pak1 or EGFR protein and then 24 h later transfected with pre-miR-7. Cells were counted at daily intervals thereafter. As shown in Figure 5, we observed that overexpression of Ack1 and Pak1 significantly rescued the cell growth by approximated 40 and 60%, respectively. However, overexpression of EGFR slightly, but not significantly increased the growth of schwannoma cells transfected with pre-miR-7. Western blots in these experimental conditions showed a markedly increase in the protein levels of Ack1, Pak1, and EGFR after infection of HEI-193 cells (data not shown). Taken together our data suggest that Ack1 and Pak1 are especially important targets of miR-7 in schwannoma cell growth.

### The expression profiles of Ack1, Pak1 and EGFR in schwannoma tissues

We next examined the levels of Ack1, EGFR and Pak1 messages in human vestibular schwannoma tumor samples. We performed qRT-PCR for the messages in 10 tumor samples used in our miRNA screening experiments as compared to the average for control nerves. Levels of miR-7 in these tumor samples were determined by qRT-PCR and normalized to U6 RNA (Fig. 6A). Interestingly, Ack1 mRNA was found to be significantly upregulated in 9 of 10 tumor samples (Fig. 6B), and a significant increase in Pak1 mRNA (Fig. 6C) was found in all tumor tissues. In contrast, EGFR mRNA was only significantly upregulated in 5 out of 10 schwannoma tumor samples compared to the controls (Fig. 6D). A significant inverse correlation was found between levels of miR-7 and that of Ack1 and Pak1 mRNAs in schwannoma tissue samples (Supplementary Fig. 5). No significant correlation was found between miR-7 downregulation and EGFR mRNA upregulation (Supplementary Fig. 5) suggesting that in schwannoma samples not all miRNA-mRNA interactions result in degradation of mRNA. These results demonstrate that miR-7 is a major regulator in schwannoma growth, by regulation of Ack1 and Pak1 expression.

## DISCUSSION

In the present study, we define a schwannoma-typical miRNA signature by miRNA microarray expression profiling of human vestibular schwannomas as compared to control nerves. This signature includes 12 miRNAs that are deregulated in most schwannoma tumor samples. Out of these 12 miRNAs, 8 were confirmed to be significantly upregulated in schwannomas (5–20-fold); and 4 miRNAs downregulated (5–12-fold). In this study, we

focused on one of the most downregulated miRNA, miR-7, and found that overexpression of miR-7 inhibited schwannoma cell growth both in culture and in xenograft and orthotopic schwannoma tumor models *in vivo.* Our studies describe a novel target of miR-7, which directly targeted the sequences in the 3'UTR of the Ack1 mRNA with upregulation of miR-7 decreasing levels of Ack1 mRNA and protein in schwannoma cells. A significant inverse correlation was also found between miR-7 downregulation and Ack1 and Pak1 upregulation in human schwannoma tumor samples compared to control nerve tissue.

The overexpression or genomic amplification of Ack1 has been recently shown for breast, esophageal, lung, ovarian, pancreatic and prostate cancer (20). In prostate cancer, Ack1 stimulates tumorigenesis in part by negatively regulating the proapoptotic tumor suppressor, the WW domain containing oxidoreductase (Wwox) (33). Ack1 interacts with Wwox and triggers its ubiquitination and degradation. The same study also elucidated an oncogenic role of Ack1 *in vivo,* with Ack1 overexpression promoting anchorage-independent growth and tumor formation *in vivo* (33). It remains to be investigated how upregulation of Ack1 by decreased miR-7 contributes to schwannoma tumorigenesis.

Based on the relative fold increase as assessed by qRT-PCR assays, the most upregulated miRNAs in schwannomas were let-7d (about 22-fold), miR-451 (about 17-fold), and miR-23b (about 15-fold). The let-7 family has been the most studied of the potential "tumor suppressor" miRNAs and contains 11 family members (reviewed in 21). This family acts as tumor suppressors to control several oncogenic pathways, including the Ras pathway (12), as well as oncogenes, such as c-Myc (34). The second most upregulated miRNA in schwannomas, miR-451 was also recently shown to function as a potential tumor suppressor in human gastric and colon cancer cells, with its overexpression decreasing proliferation and increasing response to ionizing radiation in culture (22). In human malignant prostate cancers, miR-23a and miR-23b were shown to be downregulated compared to normal prostate tissues (35). In summary, several previously known downregulated "tumor suppressor miRNAs" in malignant tumors, such as let-7d, miR-451, miR-23a, and miR-29 were found to be upregulated in schwannomas. Based on these observations and given the fact that let-7d, let-7b, and let-7g tumor suppressor miRNAs are also upregulated in benign meningiomas (13), it seems likely that these miRNAs may function as a pivotal point in tumor progression between benign and malignant states by regulating certain oncogenic pathways.

In conclusion, growth inhibitory/apoptotic effects of elevated miR-7 levels were found in human primary and immortalized schwannoma cells, as well as in a non-immortalized mouse schwannoma cell line. miRNA expression profiling and functional studies of miR-7 in schwannoma tumor tissue and cells in culture suggest that miR-7 acts as a potential tumor suppressor in schwannomas, at least in part through direct targeting of IRS-2 (15), Ack1, Pak1, and EGFR. Studies supporting a role for Pak1 (36,37), EGFR (38), and Ack1 (this study) activation/overexpression in schwannoma growth, suggests alternative strategies and rationale for the development of new therapies for these tumors based on overexpression of miR-7 or inhibition of Ack1, Pak1, and EGFR pathways. Given the fact that schwannomas, as many other cancers, are not always responsive to anti-EGFR treatment (39), our study suggests that Pak1 and/or Ack1 may prove critical therapeutic targets for schwannomas.

## Supplementary Material

Refer to Web version on PubMed Central for supplementary material.

## Acknowledgments

We thank Dr. Benjamin Purow for p3'UTR-EGFR and p3'UTR-IRS-2 plasmids and Dr. Bakhos A. Tannous for the lentivirus Fluc vector. We also thank Suzanne McDavitt for skilled editorial assistance and MGH Neuroscience Center vector core (NIH/NINDS P30NS045776) for packaging the lentivirus vectors.

**Grant support**: NIH/NINDS P01 NS24279 (XOB/OS), DOD W81XWH-09-1-0476 (XOB/OS), Children's Tumor Foundation 2007-01-043 (OS)

## References

1. Martuza RL, Eldridge R. Neurofibromatosis 2 (bilateral acoustic neurofibromatosis). N Engl J Med. 1988; 318:684–688. [PubMed: 3125435]
2. Jones GN, Tep C, Towns WH, et al. Tissue-specific ablation of Prkar1a causes schwannomas by suppressing neurofibromatosis protein production. Neoplasia. 2008; 10:1213–1221. [PubMed: 18953430]
3. Boyd C, Smith MJ, Kluwe L, Balogh A, Maccollin M, Plotkin SR. Alterations in the SMARCB1 (INI1) tumor suppressor gene in familial schwannomatosis. Clin Genet. 2008; 74:358–366. [PubMed: 18647326]
4. Evans DG. Neurofibromatosis type 2 (NF2): a clinical and molecular review. Orphanet J Rare Dis. 2009; 4:16. Review. [PubMed: 19545378]
5. Sekido Y. Genomic abnormalities and signal transduction dysregulation in malignant mesothelioma cells. Cancer Sci. 2010; 101:1–6. [PubMed: 19793348]
6. Lau YK, Murray LB, Houshmandi SS, Xu Y, Gutmann DH, Yu Q. Merlin is a potent inhibitor of glioma growth. Cancer Res. 2008; 68:5733–5742. [PubMed: 18632626]
7. Scheithauer BW, Erdogan S, Rodriguez FJ, et al. Malignant peripheral nerve sheath tumors of cranial nerves and intracranial contents: a clinicopathologic study of 17 cases. Am J Surg Pathol. 2009; 33:325–338. [PubMed: 19065105]
8. Horiguchi A, Zheng R, Shen R, Nanus DM. Inactivation of the NF2 tumor suppressor protein merlin in DU145 prostate cancer cells. Prostate. 2008; 68:975–984. [PubMed: 18361411]
9. Ambros V. The functions of animal microRNAs. Nature. 2004; 431:350–355. [PubMed: 15372042]
10. Esquela-Kerscher A, Slack FJ. Oncomirs - microRNAs with a role in cancer. Nat Rev Cancer. 2006; 6:259–269. [PubMed: 16557279]
11. Johnson SM, Grosshans H, Shingara J, et al. RAS is regulated by the let-7 microRNA family. Cell. 2005; 120:635–647. [PubMed: 15766527]
12. Takamizawa J, Konishi H, Yanagisawa K, et al. Reduced expression of the let-7 microRNAs in human lung cancers in association with shortened postoperative survival. Cancer Res. 2004; 64:3753–3756. [PubMed: 15172979]
13. Saydam O, Shen Y, Wurdinger T, et al. Downregulated microRNA-200a in meningiomas promotes tumor growth by reducing E-cadherin and activating the Wnt/{beta}-catenin signaling pathway. Mol Cell Biol. 2009; 29:5923–5940. [PubMed: 19703993]
14. Reddy SD, Ohshiro K, Rayala SK, Kumar R. MicroRNA-7, a homeobox D10 target, inhibits p21-activated kinase 1 and regulates its functions. Cancer Res. 2008; 68:8195–8200. [PubMed: 18922890]
15. Kefas B, Godlewski J, Comeau L, et al. microRNA-7 inhibits the epidermal growth factor receptor and the Akt pathway and is down-regulated in glioblastoma. Cancer Res. 2008; 68:3566–3572. [PubMed: 18483236]
16. Dummler B, Ohshiro K, Kumar R, Field J. Pak protein kinases and their role in cancer. Cancer Metastasis Rev. 2009; 28:51–63. [PubMed: 19165420]
17. Bokoch GM. Biology of the p21-activated kinases. Annu Rev Biochem. 2003; 72:743–781. Review. [PubMed: 12676796]
18. Vadlamudi RK, Kumar R. P21-activated kinases in human cancer. Cancer Metastasis Rev. 2003; 22:385–393. [PubMed: 12884913]
19. Mott HR, Owen D, Nietlispach D, et al. Structure of the small G protein Cdc42 bound to the GTPase-binding domain of ACK. Nature. 1999; 399:384–388. [PubMed: 10360579]

20. van der Horst EH, Degenhardt YY, Strelow A, et al. Metastatic properties and genomic amplification of the tyrosine kinase gene ACK1. Proc Natl Acad Sci U S A. 2005; 102:15901–15906. [PubMed: 16247015]
21. Roush S, Slack FJ. The let-7 family of microRNAs. Trends Cell Biol. 2008; 18:505–506. [PubMed: 18774294]
22. Bandres E, Bitarte N, Arias F, et al. microRNA-451 regulates macrophage migration inhibitory factor production and proliferation of gastrointestinal cancer cells. Clin Cancer Res. 2009; 15:2281–2290. [PubMed: 19318487]
23. Hung G, Li X, Faudoa R, et al. Establishment and characterization of a schwannoma cell line from a patient with neurofibromatosis 2. Int J Oncol. 2002; 20:475–482. [PubMed: 11836557]
24. Prabhakar S, Messerli SM, Stemmer-Rachamimov AO, et al. Treatment of implantable NF2 schwannoma tumor models with oncolytic herpes simplex virus G47Delta. Cancer Gene Ther. 2007; 14:460–467. [PubMed: 17304235]
25. Saydam O, Senol O, Mizrak A, et al. A novel imaging-compatible sciatic nerve schwannoma model. J Neuroscience Methods. provisionally accepted.
26. PicTar [homepage on the Internet]. Berlin: PicTar is an algorithm for the identification of microRNA targets. Available from: http://pictar.mdc-berlin.de/cgibin/PicTar_vertebrate.cgi
27. Goodwin EC, DiMaio D. Repression of human papillomavirus oncogenes in HeLa cervical carcinoma cells causes the orderly reactivation of dormant tumor suppressor pathways. Proc Natl Acad Sci U S A. 2000; 97:12513–12518. [PubMed: 11070078]
28. Thomas R, Prabhu PD, Mathivanan J, et al. Altered structure and expression of RB1 gene and increased phosphorylation of pRb in human vestibular schwannomas. Mol Cell Biochem. 2005; 271:113–121. [PubMed: 15881662]
29. Webster RJ, Giles KM, Price KJ, Zhang PM, Mattick JS, Leedman PJ. Regulation of epidermal growth factor receptor signaling in human cancer cells by microRNA-7. J Biol Chem. 2009; 284:5731–5741. [PubMed: 19073608]
30. Galisteo ML, Yang Y, Ureña J, Schlessinger J. Activation of the nonreceptor protein tyrosine kinase Ack by multiple extracellular stimuli. Proc Natl Acad Sci U S A. 2006; 103:9796–9801. [PubMed: 16777958]
31. Howlin J, Rosenkvist J, Andersson T. TNK2 preserves epidermal growth factor receptor expression on the cell surface and enhances migration and invasion of human breast cancer cells. Breast Cancer Res. 2008; 10:R36. [PubMed: 18435854]
32. Kato-Stankiewicz J, Ueda S, Kataoka T, Kaziro Y, Satoh T. Epidermal growth factor stimulation of the ACK1/Dbl pathway in a Cdc42 and Grb2-dependent manner. Biochem Biophys Res Commun. 2001; 284:4470–4477.
33. Mahajan NP, Whang YE, Mohler JL, Earp HS. Activated tyrosine kinase Ack1 promotes prostate tumorigenesis: role of Ack1 in polyubiquitination of tumor suppressor Wwox. Cancer Res. 2005; 65:10514–10523. [PubMed: 16288044]
34. Sampson VB, Rong NH, Han J, et al. MicroRNA let-7a down-regulates MYC and reverts MYC-induced growth in Burkitt lymphoma cells. Cancer Res. 2007; 15:9762–9770. [PubMed: 17942906]
35. Porkka KP, Pfeiffer MJ, Waltering KK, Vessella RL, Tammela TL, Visakorpi T. MicroRNA expression profiling in prostate cancer. Cancer Res. 2007; 67:6130–6135. [PubMed: 17616669]
36. Yi C, Wilker EW, Yaffe MB, Stemmer-Rachamimov A, Kissil JL. Validation of the p21-activated kinases as targets for inhibition in neurofibromatosis type 2. Cancer Res. 2008; 68:7932–7937. [PubMed: 18829550]
37. Kissil JL, Wilker EW, Johnson KC, Eckman MS, Yaffe MB, Jacks T. Merlin, the product of the Nf2 tumor suppressor gene, is an inhibitor of the p21-activated kinase, Pak1. Mol Cell. 2003; 12:841–849. [PubMed: 14580336]
38. Clark JJ, Provenzano M, Diggelmann HR, Xu N, Hansen SS, Hansen MR. The ErbB inhibitors trastuzumab and erlotinib inhibit growth of vestibular schwannoma xenografts in nude mice: a preliminary study. Otol Neurotol. 2008; 29:846–853. [PubMed: 18636037]

39. Plotkin SR, Stemmer-Rachamimov AO, Barker FG 2nd, et al. Hearing improvement after bevacizumab in patients with neurofibromatosis type 2. N Engl J Med. 2009; 361:358–367. [PubMed: 19587327]

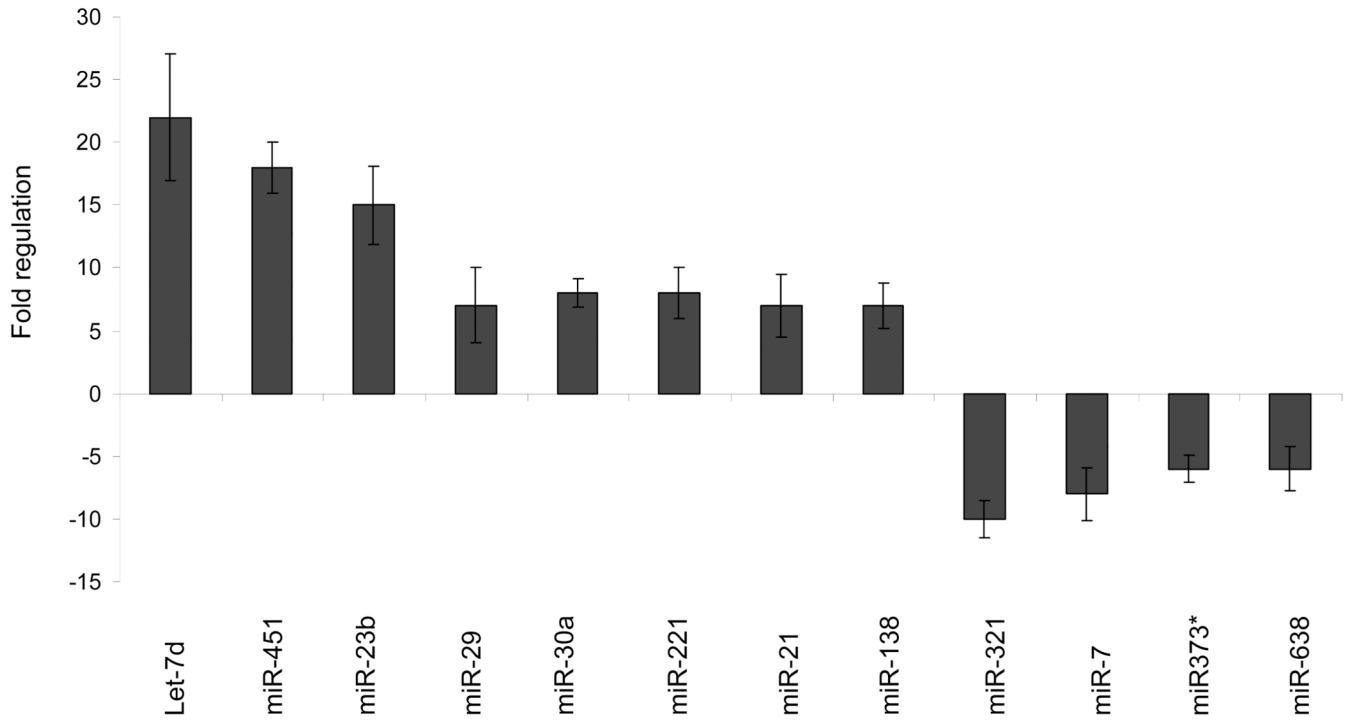


**Figure 1. miRNA signature of schwannomas**

miRNA expression profiles of human vestibular schwannomas were compared with peripheral nerve tissue controls. miRNA screening was performed in duplicate for 10 tumor and 2 control samples by microarray analysis. (Supplementary Table 1). To validate the deregulated miRNAs, we also performed multiplex RT-PCR using 4 control and 10 randomly selected tumor samples. The data were normalized to the level of U6 RNA in each sample. Twelve validated up and downregulated miRNAs values are shown as the mean ± S.D. relative to the control mean (***$p<0.0001$, Student's *t*-test).

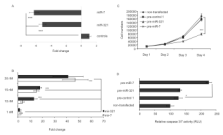

**Figure 2. Gain-of-function studies of downregulated miRNAs on schwannoma cell growth**

(A): qRT-PCRs for miR-321, miR-7, and U6 were performed in low MW fraction of RNA isolated from HEI-193 schwannoma cells and normalized to the level of U6 RNAs in each sample. (B): Two days after transfection of HEI-193 cells with pre-miR-321 or pre-miR-7, RNA was isolated and qRT-PCR reactions were performed for miR-321 and miR-7 normalized to U6. (C): HEI-193 cells were either transfected with pre-miR-321, pre-miR-7 or pre-control 1, or non-transfected and seeded in each well of a 6-well plate 5 h after transfection. Cells were counted at 1, 2, 3, and 4 days after transfection. (D): To determine the apoptosis rate in experiment shown in panel C, Caspase-Glo 3/7 (Promega) assay was carried out on cell lysates 2 days after transfection and expressed as RLU. These experiments were performed in triplicate and the values are expressed as mean ± S.D. (*p<0.02 ***p<0.0001 Student's *t*-test).

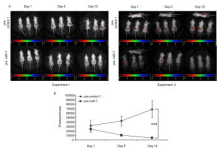

**Figure 3. miR-7 inhibits schwannoma tumor growth *in vivo***

HEI-193-Fluc-mC cells were transfected with either pre-miR-7 or pre-control 1 and implanted subcutaneously into the flanks of 5-week-old female athymic mice (nu/nu) five h later (7 mice per group). Tumor growth was monitored by *in vivo* bioluminescence imaging using a CCD camera. (A): This experiment was performed twice and bioluminescent images are shown with a pseudocolor bar to indicate degree of bioluminescence at 1, 5 and 10 days after tumor cell implantation. (B): Relative luciferase activity is shown as the mean ± S.D. (***p<0.0001; pre-miR-7 versus pre-control 1, Student's *t*-test.

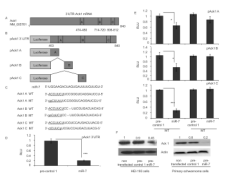

**Figure 4. Identification of miR-7 binding sites in the 3'UTR of the Ack1 mRNA**

(A): Schematic representation of the Ack1 mRNA with three 3′UTR miR-7 binding sites (A, B, and C), as predicted by Pictar. (B): Schematic representation of Fluc reporter vectors for miR-7 target sites, partial wt pAck1 3′UTR containing all three putative binding sites (453–840 nt), and partial Ack1 3′UTRs containing sites pAck1 A, pAck1 B or pAck1 C. (C): The mature miR-7 sequence with its binding sites and wt and mt (mt, lower case) forms of the Ack1 mRNA 3′UTR miR-7 target sites are shown. (D): The pMiR-Report vector containing all three binding sites in the 3'UTR of the Ack1 mRNA with pre-miR-7 or pre-control 1, and an expression cassette for Rluc, were co-transfected into HEK 293T cells. Two days later, Fluc activity in the cells was measured and normalized to Rluc activity. (E): In a similar experiment, pMIR vectors containing pAck1 3'UTR sites A, B or C and their mutated counterparts were co-transfected into HEK 293T cells and luciferase activities were measured, as above. These experiments were performed in triplicate and results are shown as the mean ± S.D. (*p<0.01, ***p<0.001, Student's *t*-test). (F): HEI-193 cells were transfected either with pre-control 1 or pre-miR-7 and three days after transfection, western blots were performed for Ack1 and actin (one of two similar blots is shown).

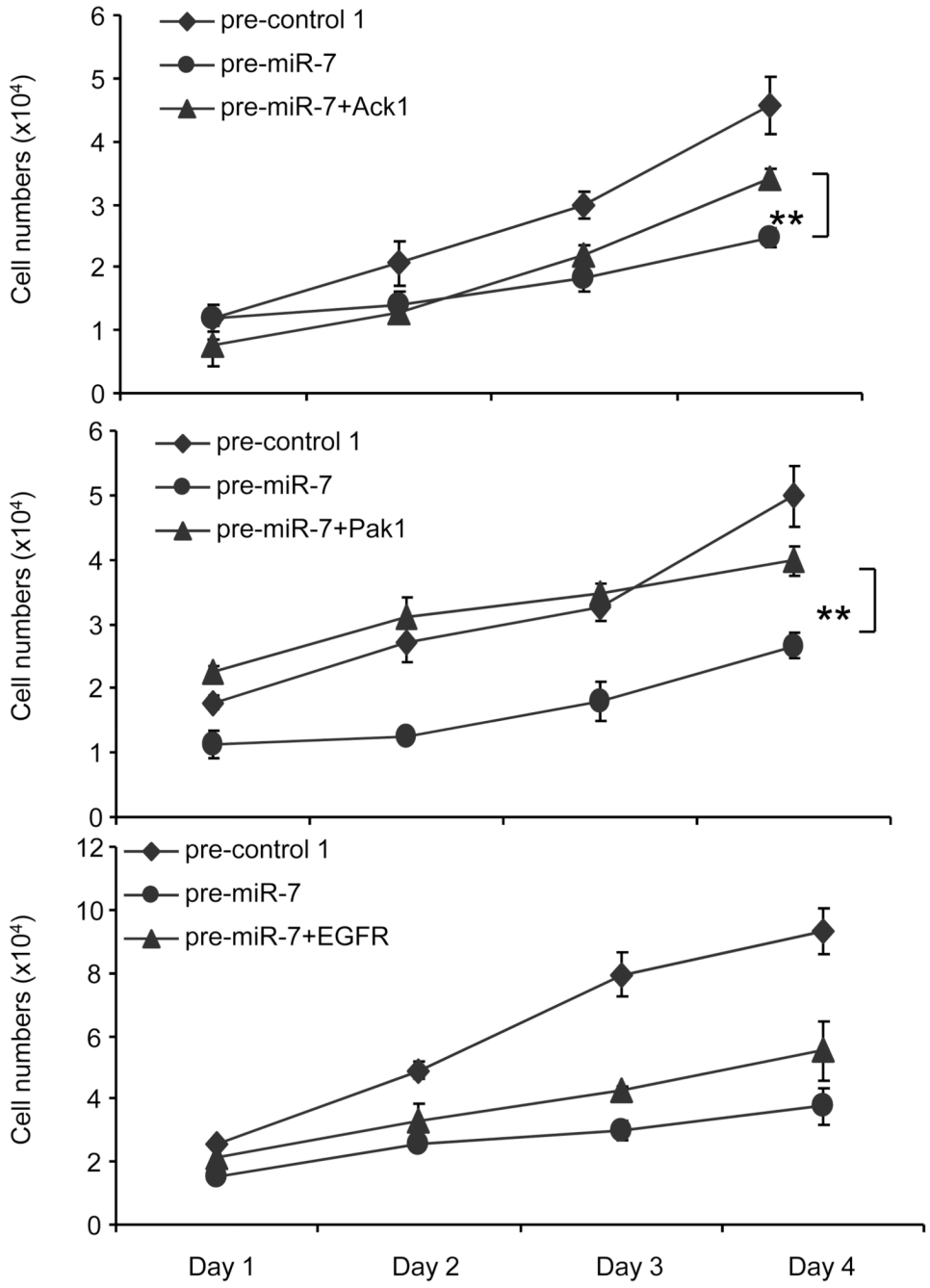


**Figure 5. Ack1 and Pak1 are important targets of miR-7 in schwannoma cell growth**

HEI-193 cells were first infected with viral vectors expressing Ack1 or Pak1 or EGFR and then 24 h later transfected with pre-miR-7. Cells were counted at daily intervals thereafter. These experiments were performed in triplicate and results are shown as the mean ± S.D. (**p<0.01, Student's *t*-test).

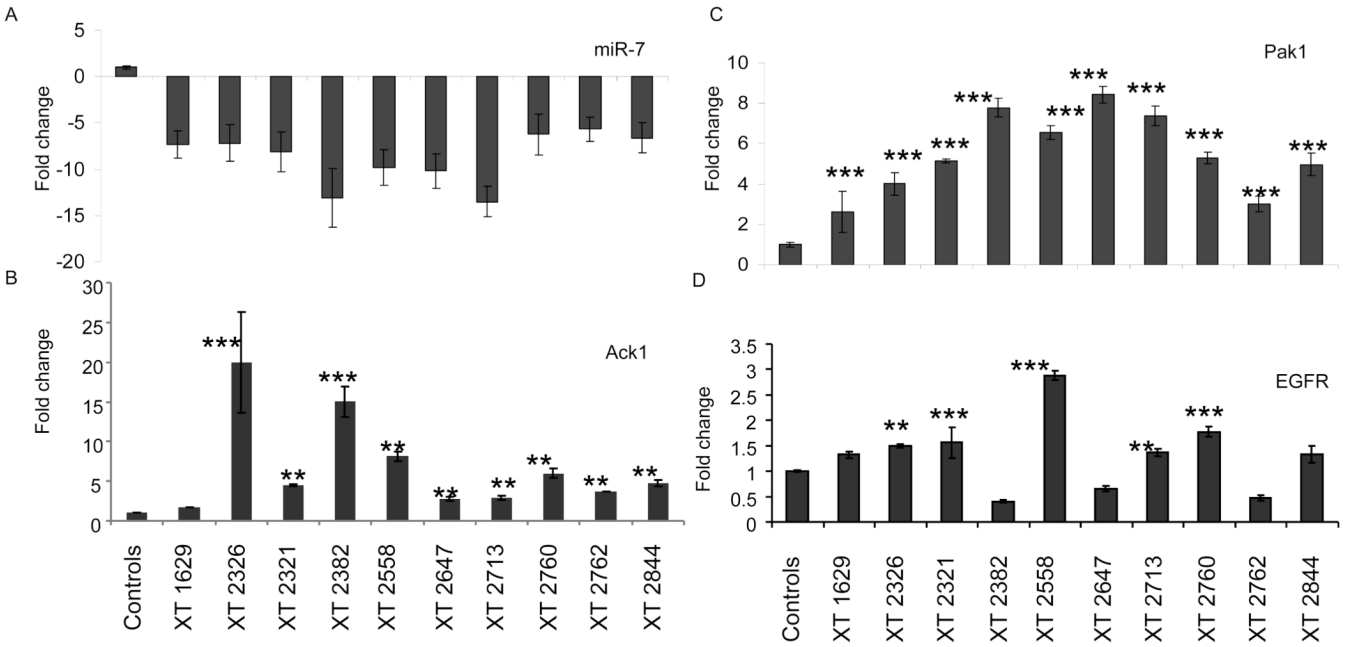


**Figure 6. miR-7 levels correlate with expression of Ack1 and Pak1 mRNAs**

qRT-PCR reactions were performed in 10 schwannoma tumor and 2 control samples for miR-7 and U6 (A), Ack1 mRNA (B), Pak1 mRNA (C) and EGFR mRNA (D), and normalized to GAPDH mRNA. These experiments were performed in triplicate and results are shown as the mean ± S.D. (***p<0.001, **p<0.01, Student's *t*-test).